Electronic Supplementary Material (ESI) for Journal of Materials Chemistry A.

Supporting Information for:

Vulcanization Accelerator Enabled Sulfurized Carbon Material for High Capacity High Stability Lithium-Sulfur Batteries

Hongwei Chen,[a,†] Changhong Wang,[a,†] Chenji Hu,[a,b,†] Jiansheng Zhang,[a] Shan Gao,[a] Wei Lu[a] and Liwei Chen[a,*]

[a] i-LAB, Suzhou Institute of Nano-Tech and Nano-Bionics (SINANO), Chinese Academy of Sciences, Suzhou 215123, China

[b] College of Sciences, Shanghai University, Shanghai 200444, China

† These authors contributed equally to this work

* To whom correspondence should be addressed: lwchen2008@sinano.ac.cn

Experimental section

a) Chemicals and materials

Sulfur powder (99.9%), 2-mercaptobenzothiazoles, and polyacrylonitrile (Mw=150,000) were purchased from Aldrich. Toluene (analytical grade) was purchased from Sinopharm Chemical Reagent Co., Ltd. The reagents were used as purchased without purification or treatment.

b) Synthesis of PAN-S and PAN-S-VA

The mass ratio of PAN: S=1:1 and PAN: S: VA=1:1:0.1 was used for the synthesis of PAN-S and PAN-S-VA, respectively. The reactants were mixed with ground milling; then the mixture was sealed and heated under argon at a rate of 10 °C /min up to 180 °C. The mixture was kept at 180 °C for 1h and further heated up to 280 °C, and kept at 280 °C for another 6h. The as-prepared compounds were rinsed with toluene for no less than three times to remove any remaining sulfur.

c) Battery assembly and testing

The sulfurized carbon compound prepared with or without VA, i.e. PAN-S and PAN-S-VA, were mixed with acetylene black and LA132 (as the binder) with mass ratio 80:10:10 to prepare the cathode. The Coin-type (CR2025) cells were fabricated by sandwiching a porous polypropylene separator between a cathode containing the active materials and a lithium metal foil in a high-purity argon-filled glove box to avoid moisture and oxygen contamination. The electrolyte used was 1.0 M $LiPF_6$ in a solvent mixture of EC/DMC (1:1 v/v). The cells were discharged and charged on a battery test system (NEWARE, NEWARE technology Ltd. Shenzhen) from 1.0 to 3.0 V at a current density of 400 mA /g unless specifically noted.

d) Materials characterization

The as-prepared samples were characterized using a Scanning Electron Microscope (SEM) (FEI Quanta 400 FEG). Transmission electron microscope (TEM) images were recorded using a Tecnai G2 F20 S-TWIN equipped with energy dispersive X-ray microanalysis (EDX) at 200 kV. The XPS were recorded using Thermo Scientific ESCALAB 250Xi with Al Kα-radiation. Raman spectra were recorded using a Jobin Yvon LabRam HR 800 confocal micro-Raman system. Sulfur content of the samples was analyzed using an elemental analyzer (CHNS, Vario EL Cube, Elementar), and the vendor specified uncertainty of the elemental analysis measurements is within ±0.01%. The AC impedance of freshly prepared cells was measured at the open circuit potential (OCP), using an AutoLab electrochemical workstation (PGSTAT302N). The AC testing voltage amplitude was ±5 mV, and the frequency ranged from 100 kHz to 0.1 Hz.

Supplemental results and discussion

a) Reactions of PAN, sulfur, and VA

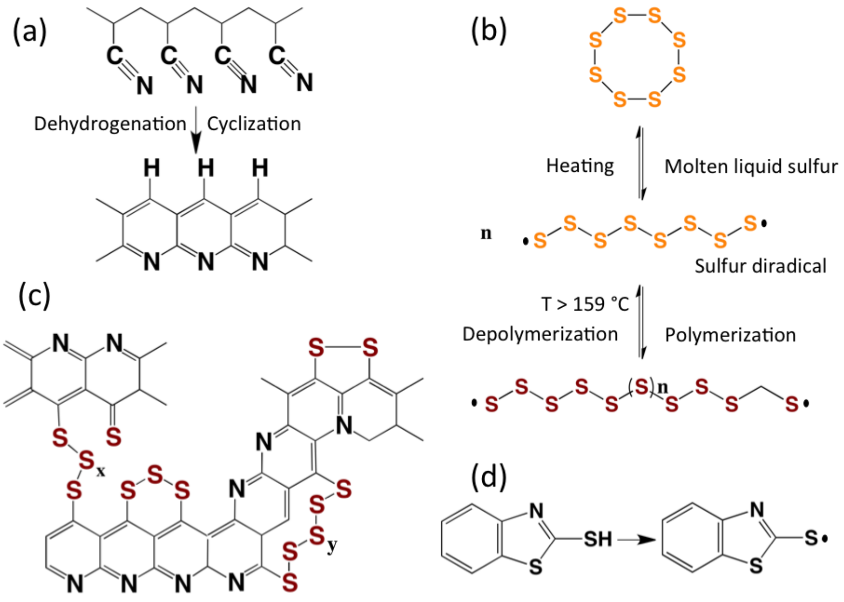

Scheme S1. (a) Dehydrogenation and cyclization of PAN with increasing temperature,[1] including: 1) dehydrogenation and cyclization into a ladder-structural polymer by the mild oxidization in the 300–400°C range; 2) deamination to form a ribbon-structural polymer in the 400–600°C range, and 3) carbonization and further graphitization above 600°C.[2] (b)

Schematic of sulfur converting into polysulfides under increasing temperature. Elemental sulfur under ambient conditions exists primarily in the form of an eight-membered ring (S_8) that melts into a clear yellow liquid phase at ~120°C. Rings with 8–35 sulfur atoms are formed and further heating of the liquid sulfur phase above 159°C results in equilibrium ring-opening polymerization (ROP) of the S_8 monomer into a linear polysulfide with diradical chain ends.[3, 4] (c) Proposed chemical structure of sulfurized PAN cited from ref. 5 ($0 < x < 6$; $y = 1,2$).[5] The short polysulfide chains are covalently bonded to the cyclized and dehydrogenated PAN backbones through the C–S bonds. It should be note that the chemical structure and electrochemical properties of PAN-S have been poorly understood. There are some excellent published papers focused on the understanding of the unsettled problems.[2, 6, 7] (d) 2-mercaptobenzothiazole (the VA used in this work) decomposes into active radical at high temperature.[8, 9]

b) Elemental analysis

	C [wt%]	H [wt%]	S [wt%]
PAN-S	45.78	0.99	28.47
PAN-S-VA	40.01	0.87	36.89

c) TEM and EDX

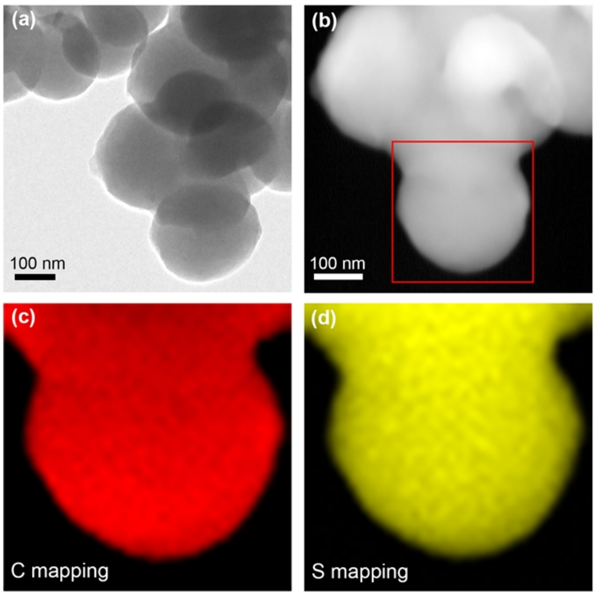

Figure S1. (a) TEM image of PAN-S-VA. (b-d) Elemental mapping of C and S under STEM mode.

d) Normalized rate performances of PAN-S and PAN-S-VA

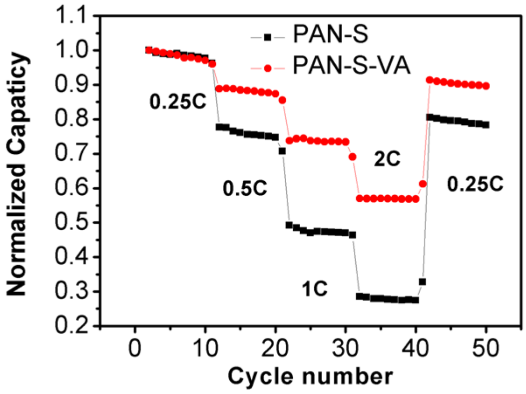

Figure S2. Normalized rate performances of PAN-S and PAN-S-VA based on Fig.4c in the manuscript.

The normalized cycling performances of PAN-S and PAN-S-VA based on Fig.4c (discard the 1st discharge capacity) were compared. As shown in Figure S2, the PAN-S-VA sample actually display better rate than PAN-S, especially at high rates of 0.5C or 1C.

e) Raman spectra of PAN-S and PAN-S-VA

Raman spectra of PAN-S and PAN-S-VA are shown in Figure S3. For carbon materials, the D band (~1360 cm^{-1}) indicates the presence of defects and the G band (~1575 cm^{-1}) reflects the graphitic order. The intensity ratio of D to G band (I(D) / I(G) or I(D) / I(D) + I(G)) has been largely used as a reference disorder parameter of the structure.[10, 11] Compared with the PAN-S, the Raman spectrum of PAN-S-VA shows a higher I(D) / I(G) ratio, indicating lower degree of graphitization (i.e. more disorder structure) in PAN-S-VA. In addition, the D band of PAN-S-VA is shifted towards lower wave number, which can be attributed to a stronger amorphous character of PAN-S-VA with respect to graphite.[5]

Although the nature of the interactions between lithium and organosulfide-carbon are still unclear, we can qualitatively understand the EIS results based on the model proposed by Y. Matsumura et.al. for the interactions between disordered carbon and lithium.[12] In this model, lithium ions locate not only between graphitic layers, but also at the edge of graphitic structures and on the surface of crystallites. Analogously, lithium ions may interact with various different sites in sulfurized PAN due to the amorphous structure with unique semigraphitic layers. The higher degree of disorder in PAN-S-VA may thus facilitate faster lithium ion diffusion than that in PAN-S, and thus allow for low charge transfer resistance as reflected in the EIS spectra.

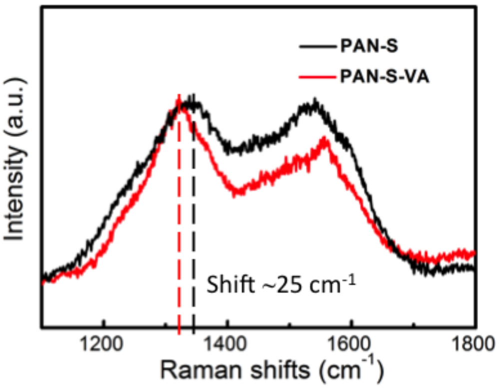

Figure S3. Raman spectra of PAN-S and PAN-S-VA at the 1100-1800 cm^{-1} range.

References

1. M. Rahaman, A. F. Ismail and A. Mustafa, *Polymer Degradation and Stability*, 2007, **92**, 1421-1432.
2. S. S. Zhang, *Frontiers in Energy Research*, 2013, **1**, 10.
3. B. Meyer and N. Kharasch, 1965.
4. W. J. Chung, J. J. Griebel, E. T. Kim, H. Yoon, A. G. Simmonds, H. J. Ji, P. T. Dirlam, R. S. Glass, J. J. Wie and N. A. Nguyen, *Nature chemistry*, 2013, **5**, 518-524.
5. J. Fanous, M. Wegner, J. Grimminger, A. n. Andresen and M. R. Buchmeiser, *Chemistry of Materials*, 2011, **23**, 5024-5028.
6. S. S. Zhang, *Energies*, 2014, **7**, 4588-4600.
7. J. Wang, Y. S. He and J. Yang, *Advanced Materials*, 2014.
8. P. Ghosh, S. Katare, P. Patkar, J. M. Caruthers, V. Venkatasubramanian and K. A. Walker, *Rubber chemistry and technology*, 2003, **76**, 592-693.
9. M. Krejsa and J. Koenig, *Rubber chemistry and technology*, 1993, **66**, 376-410.
10. M. Matthews, M. Pimenta, G. Dresselhaus, M. Dresselhaus and M. Endo, *Physical Review B*, 1999, **59**, R6585.
11. J. Fanous, M. Wegner, J. Grimminger, M. Rolff, M. B. Spera, M. Tenzer and M. R. Buchmeiser, *Journal of Materials Chemistry*, 2012, **22**, 23240-23245.
12. Y. Matsumura, S. Wang and J. Mondori, *Carbon*, 1995, **33**, 1457-1462.